Multiple bandwidth volumetric optoacoustic tomography using conventional ultrasound linear arrays

Andrei Chekkoury¹, Jérôme Gateau and Vasilis Ntziachristos

Institute for Biological and Medical Imaging (IBMI), Technische Universität München and Helmoholtz Zentrum München, Ingolstädter Landstraße 1, 85674, Neuherberg, Germany

ABSTRACT

In optoacoustic imaging absorbing structures excited with short laser pulses generate broadband ultrasound waves, which tomographically detected outside the sample enable reconstruction of initial pressure distribution. As light scatters in biological tissues, the excitation has a three-dimensional (3D) pattern allocation. Accurate reconstruction of the 3D distribution of optical absorption requires a large solid angle of detection of the ultrasonic field. Moreover, the center frequency and bandwidth of a given detector define the range of structure sizes it is able to resolve. Therefore, detectors with different frequency bandwidths record different subsets of information. A volumetric optoacoustic system using linear ultrasound arrays with different central frequencies, 6MHz and 24MHz, is introduced. By employing a novel scanning geometry that takes advantage of the high sensitivity on the transversal dimension of these linear probes, high resolution optoacoustic signals are being recorded. Resolution performance and biological capabilities are demonstrated with a 20um crossed-suture phantom and an excised mouse liver lobe.

Keywords: Optoacoustic tomography, Photoacoustic imaging, Photoacoustics, Ultrasound

1. INTRODUCTION

Optoacoustic (photoacoustic) tomography is a biomedical imaging modality that can provide high-resolution mapping of optical absorption up to a few centimeters depth in tissue ¹. This modality can therefore be used to image vasculature due to the high optical absorption contrast between vessels and tissue in the near infrared region. Optoacoustic imaging relies on detection of ultrasonic waves generated by the thermoelastic expansion of absorbing structures after high-energy laser pulse illumination of the sample. Due to light scattering in biological tissues, the optical excitation is volumetric. To be able to reconstruct this volumetric distribution of optical absorption, a tomographic detection, where ultrasound detectors are distributed on a surface surrounding the sample, can be used. The induced ultrasound waves are broadband and with peak frequency corresponding to different object sizes ². The central frequency and bandwidth of a given detector define the range of structure sizes that it is able to resolve. Therefore, detectors with different frequency bandwidths will record different subsets of information.

In the current work, we present a three-dimensional (3D) tomographic system using conventional ultrasound arrays of different bandwidths in a rotation/translation scan geometry ³. Two different arrays of different central frequencies, 6MHz and 24MHz respectively, were used here. The system allows successive acquisitions of volumetric images of the same sample with the two arrays, and therefore enables to obtain high resolution images at different scales. Each frequency band allows resolving in 3D different structures of the sample. A similar approach, involving optoacoustic scanning using transducers with different bandwidths, was previously introduced in ⁴ with a circular scan of single-element transducers cylindrically focused perpendicularly on the rotation axis. This approach was, however, limited by the ability to only produce two-dimensional images, and by the integration of signals originating from a large slice thickness.

In this study, our system was first characterized with a phantom comprised of two 20 µm diameter black threads arranged in a cross, and its capabilities to resolve structures in a large range of scales are shown through images of an *ex vivo* excised portion of a mouse liver.

Opto-Acoustic Methods and Applications, edited by Vasilis Ntziachristos, Charles P. Lin, Proc. of OSA Biomedical Optics-SPIE Vol. 8800, 880003 · © 2013 OSA-SPIE CCC code: 1605-7422/13/\$18 · doi: 10.1117/12.2032064

¹ E-Mail: andrei.chekkoury@gmail.com

2. MATERIALS AND METHODS

The experimental setup consisted of three main components: 1) the excitation part, comprised of a nanosecond pulsed laser and a fiber bundle, 2) the ultrasonic detection containing two linear arrays with different central frequencies together with two data acquisition systems, and 3) the array holder with motorized translation and rotation stages. The array and phantom holder were immersed into water for proper acoustic coupling.

The optical excitation of the samples was performed using a tunable (690-900nm) optical parametric oscillator laser (Phocus II, Opotek Inc., Carlsbad, California), delivering <10ns duration pulses with a repetition rate of 10Hz. The beam was guided into a silica fused-end fiber bundle (CeramOptec GmbH, Bonn, Germany) consisting of 640 fibers partitioned into 4 legs. The Laser was tuned at 760nm, and delivered a per-pulse energy of 70mJ at the laser's output.

The acoustic detection was performed using two ultrasonic arrays: one low frequency commercially available linear array (5.0/7.0 MHz, Acuson L7, Siemens Healthcare) and one high frequency (24 MHz center frequency, Vermon, Tours, France). Both arrays were designed for ultrasonography imaging and were comprised of 128 detection elements, cylindrically focused using acoustic lenses, at ~19mm and ~7.5mm, respectively. The arrays have an f-number of 4.75 and 5, respectively, considered to be a weak focus on the transversal dimension. Two custom build data acquisition systems with 128 channels allowed acquisition in parallel on all the detectors of the arrays.

A rotation/translation scan geometry was used in this experimental. This geometry was introduced in ³ for linear ultrasound array and takes advantage of the large aperture of the arrays in the longitudinal (z axis) dimension. This dimension also corresponds to the rotation axis. The focusing of the arrays in the two other dimensions (x- and y- axes) improves the detection sensitivity but, for high resolution imaging of samples larger than the focal spot, this focusing needs to be compensated for by translating the array tangentially to the rotation circle.

Employing this scanning geometry allowed encompassing large three-dimensional objects to obtain accurate volumetric reconstructions. The parameters selected were: the rotation, which covered 120 positions of a total angle span of 180° (1.5° angular step) and a total translation range of 8mm with 1.5mm steps was chosen for the low-frequency array and a 6mm range with 0.3mm steps for the high-frequency probe. Averaging 5 times for the obtained signals, the required acquisition time for the low frequency scan was 13 minutes and 29 minutes, respectively.

The characterization of the system used turbid phantoms mimicking the optical scattering properties and the speed of sound of soft tissues that were prepared by mixing 1.6% agar gel (Agar for microbiology, Fluka analytical) with 0.8% intralipid-20%(Sigma). A similar approach was used in creating a supporting medium for the excised liver sample. A modified filtered back projection algorithm⁵ was used in order to reconstruct the volumetric images. During the post-processing step, noise removal was performed by filtering the recorded signals with a bandpass filter (Butterworth, order 3) between 500 kHz and 12 MHz, for the low frequency array, and between 2MHz and 40MHz for the high frequency probe.

3. RESULTS AND DISCUSSION

For characterization of the system, a first phantom, containing a black nylon suture threads (diameter $\sim 20 \mu m$, Vetsuture, Nylon, non-absorbable Monofilament) arranged in a cross along the length of the cylindrical phantom, was imaged. This phantom allowed studying the image resolution in the sense of the Sparrow criterion. Figure 1(a) and 1(d) show the maximum amplitude projection (MAP) along the y-axis, demonstrating the advantage of the scanning geometry in term of the large field of view especially along the longitudinal direction (z axis). The field of view along the z-axis is different for the two arrays because of the individual array's aperture dimension. Figure 1(b) and Figure 1(e) present the 2D slices indicated by the red lines in Figure 1(a) and Figure 1(d) and selected close to the junction points of the two sutures. In order to assess the resolution in terms of object separability these slices were chosen when the saddle point starts to form. The distance between the two red dotted points - plotted on the maxima that correspond in the images to the two sutures - is determined to be 180 μ m for low frequency (6MHz) array and 43 μ m for the high frequency (24MHz) array. Due to the position of the ultrasound detectors in this experiment, a limited view effect is expected to lower the resolution along the z-axis. Therefore the in-plane resolution found here is expected to be lower than with point like objects. However, these values are on the same order as the optimal theoretical resolution (0.8 λ _c)⁶ and for the low frequency array in agreement with the values found in a previous study³. Figure 1(c) and 1(f) show a x-y slice away from

the cross junction. These figures illustrate that the position of the two threads can be well determined in the *xy*-plane, and show the two sutures as two round objects. The isotropic resolution in the *xy*-plane is a result of the employed scanning geometry, involving a series of translations for each rotation position of the detector.

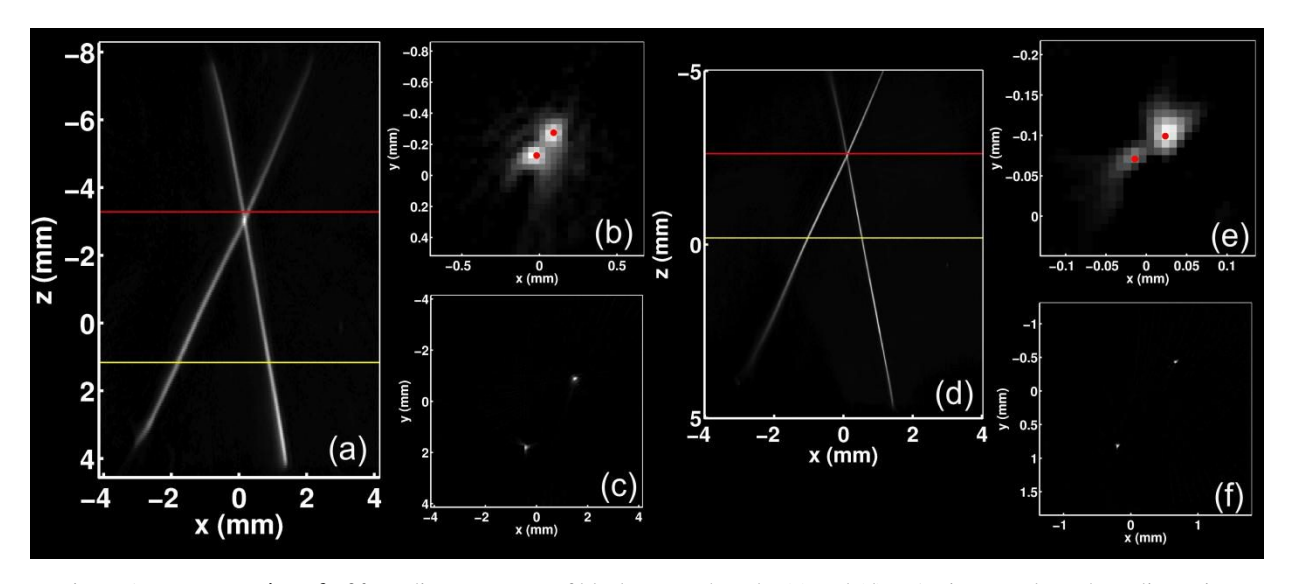


Figure 1: Reconstruction of a 20µm diameter cross of black suture threads. (a) and (d) MAP images along the y dimension respectively for the low frequency array and the high frequency. (b) and (e) reconstructed plane indicated by the red plane in (a) and (d) respectively. (c) and (f) reconstructed plane indicated by the yellow plane in (a) and (d), respectively

An excised portion of the liver of a CD1® mouse (Charles River Laboratories, Research Models and Services, Germany GmbH), was imaged with the two arrays and the corresponding MAP images are presented in Figure 2(a) and (b). The vasculature of the liver can be visualized due to the absorption of the hemoglobin at the optical wavelength of the excitation. Figure (2) shows with high accuracy the correspondence between the low frequency (a), the high-frequency (b) imaging and the post-scan photo (c). The anatomical shape of the liver lobe can be distinguished from both scanning modalities; moreover the main blood vessel (indicated by a yellow arrow) connecting the caudate lobe and other several small blood vessels that can be observed in the low frequency images are presented with a higher resolution in the high-frequency generated images.

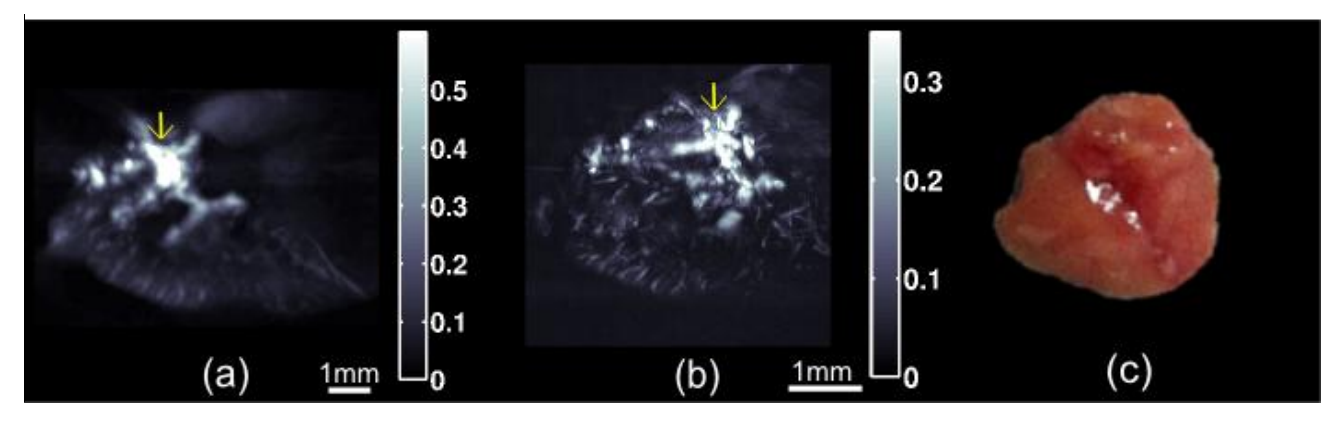


Figure 2: Excised mouse caudate liver lobe; (a) MAP image along z direction acquired with 5.0/7.0 MHz array (b) MAP image along z direction acquired with 24MHz array (c) Photo of the excised organ

4. CONCLUSION

Different biological applications require imaging anatomical structures of a wide range of shapes and sizes distributed in 3D space, i.e. the structures of a tumor and especially the microvasculature. In the current work, we presented a high-resolution system being able to generate 3D images of phantoms and biological tissues. We successfully show that by using different central frequency transducers we are able to obtain images of the same sample with different resolution and field of view. Moreover, recording the frequency spectrum of optoacoustic signals generated by different sized anatomical structures allowed obtaining images with different scales of details.

These results demonstrate that our system can be used to obtain 3D optical contrast images of biological tissues, and to coregister multiple bandwidths. Such a system will enable to focus on the general localization of a specific structure, and also on specific details at higher resolution that might reveal a distinct pathology. Moreover, multispectral approaches with such a system could provide valuable information on the volumetric localization of biomarkers and will be investigated in the near future.

5. References

- [1] V. Ntziachristos, "Going deeper than microscopy: the optical imaging frontier in biology", in Nature methods, 7(8): p. 603-614. (2010)
- [2] G. Diebold and T. Sun, "Properties of photoacoustic waves in one, two, and three dimensions", in Acta Acustica united with Acustica, 80(4): p. 339-351. (1994)
- [3] J. Gateau, et al., "Three-dimensional optoacoustic tomography using a conventional ultrasound linear detector array: Whole-body tomographic system for small animals", in Medical Physics, 40(1): p. 013302. (2013)
- [4] G. Ku, et al., "Multiple-bandwidth photoacoustic tomography", in Physics in medicine and biology, 49(7): p. 1329. (2004)
- [5] M. Xu and L.V. Wang, "Universal back-projection algorithm for photoacoustic computed tomography", in Physical Review E, **71**(1): p. 016706. (2005)
- [6] M. Xu and L.V. Wang, "Analytic explanation of spatial resolution related to bandwidth and detector aperture size in thermoacoustic or photoacoustic reconstruction", in Physical Review E, 67(5): p. 056605. (2003)